

RESEARCH ARTICLE

An Edge Preservation Index for Evaluating Nonlinear Spatial Restoration in MR Images

Justin Joseph¹, Sivaraman Jayaraman^{2*}, R. Periyasamy¹ and V.R. Simi³

¹Department of Biomedical Engineering, National Institute of Technology, Raipur-492010, India; ²Department of Biomedical Engineering, Vel Tech Multi Tech, Chennai-600062, India; ³Department of Computer Science & Engg., KVM College of Engineering & Information Technology, Alappuzha, Kerala – 688527, India

Abstract: **Background:** Edge preserving filters are widely preferred for medical image denoising as they do not degrade the morphological edges during smoothing. Even though, the operational parameters of these filters have crucial influence on their performance, the parameters are selected subjectively. The optimum values of the operational parameters can be selected objectively with the help of edge quality indices. The available edge quality indices either do not comply with the subjective quality ratings or they are prone to noise level.



Sivaraman Jayaraman

Objectives: (a) To formulate an edge preservation metric which has good correlation with subjective fidelity ratings and is robust to noise (b) To demonstrate an objective method for the selection of optimum values of the operational parameters of the non-linear spatial filters using the newly formulated edge preservation metric.

Methods: Pratt's Figure of Merit (PFOM) between the binary edge maps of the original and restored images, extracted via gradient based threshold, is used as the measure of extent to which edges are preserved during restoration. Magnetic Resonance (MR) images filtered by anisotropic diffusion for different values of number of iterations are used as ground truth images. The PFOM is compared with existing edge quality indices in terms of robustness to noise and correlation with subjective fidelity ratings.

Results: PFOM exhibits a correlation of 0.9998 with the subjective edge quality rating which is only 0.9802 for Edge Preservation Index (EPI).

Conclusion: The proposed index is robust to noise level and useful for optimizing the performance of non-linear spatial filters.

Keywords: Edge preservation index, Edge quality index, Image quality analysis, Pratt's figure of merit, non-linear restoration.

1. INTRODUCTION

Rician distributed noise originating from the inhomogeneity of magnetic field is one of the major factors which degrades the quality of Magnetic Resonance (MR) images [1, 2]. The presence of noise in the MR image decreases the accuracy of edge based techniques for automated tumor segmentation and extraction of brain region. Traditional restoration wipes off fine textural information and morphological boundaries, which may have some diagnostic value, along with the noise [3]. Different from the traditional filters, Edge Preserving Spatial Filters (EPSF) remove noise without affecting edges and textural content [4]. However, the performance of EPSFs depends on the selection of their operational parameters. The usual practice of selecting optimum

values of the operational parameters through trial and error is subjective and time consuming [5, 6]. Even though, objective methods for the identification of optimum values can be framed making use of edge quality indices, an index which can serve this purpose is not known to be available [7]. Zhang *et al.* [8] and Gomez *et al.* [9] had pointed out the lack of criteria for the objective evaluation of denoising and for the comparative evaluation of different EPSF schemes.

The indices so far reported in literature for the objective evaluation of denoising filters include Homogeneity Mean Difference (HMD) [8], ‘ $\alpha\beta$ -ratio estimator’ [9] Homogeneity Mean Error (HME) [10], Despeckling Structure Loss (DSL) [11], Despeckling Evaluation Index (DEI) [12] and a composite frequency domain index [13], formed from the mean preservation index, isotropy index and peak side lobe ratio of the energy spectrum of homogenous regions in the original image. HMD [8], HME [10] and DEI [12] characterize the homogeneity of restored images but do not account for the

*Address correspondence to this author at the Department of Biomedical Engineering, Vel Tech Multi Tech Engineering College, Chennai 600062, India; Tel: +919840968282; E-mail: mountshiva@gmail.com

extent to which edges are preserved. But, the indices meant for the parameter optimization of edge preserving filters should be able to quantify the degradation of edge quality rather than the homogeneity. The ‘ $\alpha\beta$ -ratio estimator’ proposed by Gomez *et al.* [9] is a no reference index. While assessing the quality of edge content in the restored image, the original image prior to denoising can be used as the reference. So that edge based full reference Image Quality Analysis (IQA) models are suitable for the parameter optimization of EPSFs than no reference or reduced reference models. DSL metric introduced by Yang *et al.* [11] needs noise-free reference with clearly apparent structural information, which is practically not available. In the non-linear restoration of MR images, what is available as the reference is the noisy MR image. The composite index proposed by Dellepiane and Angiati [13] seems to be computationally intense as the computations are performed in transformed domain. Perhaps, it could be more intense than the EPSF algorithm itself. Moreover, the methods available in literature [8-13] suggest the objective methods for panoramic images, mostly Synthetic Aperture Radar (SAR) images, rather than medical images.

One may think that popular IQA indices can be employed to measure the edge preservation offered by EPSFs. But, popular IQA metrics such as Mean Square Error (MSE), Signal-to-Noise Ratio (SNR), PSNR, Feature Similarity Index (FSIM) [14] and Structural Similarity Index Metric (SSIM) are similarity measures between the reference and processed images and do not specifically reflect similarity of edge content. MSE and PSNR do not correlate well with the subjective fidelity ratings [14]. Universal Quality Index (UQI) [15] is inferior to SSIM as SSIM is its improved version. Among the indices, only SSIM and FSIM has a standard dynamic range between 0 and 1 and the former three indices have no finite limit so that judging the similarity from the numerical values is difficult and are useful for mere comparison of different processing methods. However, SSIM is not superior in its performance on blurred and noisy images [16-20]. Edge Preservation Index (EPI) [21-25] is a statistical index nowadays in common use. In EPI, Laplacian kernel is used to produce the binary edge maps of the contextual and reference images. Laplacian exaggerate noise and detect negligibility weak edges also. Consequently, EPI is sensitive to noise level.

It is coherent from the literature review that, an objective method for evaluating the edge preservation capability of non-linear filters in medical images is not reported so far and most of the IQA as well as edge quality indices do not have a standard dynamic range, do not match with the subjective quality ratings and are sensitive to noise. The purpose of this study is to (a) formulate an edge quality index based on Pratt’s Figure of Merit (PFOM) which is robust to noise, has good dynamic variability and correlation with subjective quality ratings and to (b) demonstrate an objective method to quantify the extent to which the edges are preserved during non-linear image restoration, using the proposed edge quality index. The forthcoming discussions progress through the mathematical formulation of PFOM, PSNR, SSIM and the gradient based threshold which is used to extract binary edge map of original and restored images. Eventually, the ability of the proposed edge quality index to quantify the edge deg-

radation is compared with PSNR, SSIM, EPI and Subjective quality ratings.

2. MATERIALS AND METHODS

The proposed PFOM based edge quality index, EPI, SSIM and PSNR are computed between the noisy and the MR images filtered via Anisotropic Diffusion (AD). In AD filter the degree of smoothening and thereby, blurring of edges increase with number of iterations. To produce restored images of different edge quality, noisy MR image is filtered with AD with different values of number of iterations between one and ten. Other operating parameter of AD filter, the threshold of gradient modulus was maintained constant at 15. It has been subjectively confirmed that this parameter setting offers restored images with appreciable visual quality. PFOM, EPI, PSNR and SSIM are computed between original and restored images at each value of the number of iterations. The binary edge maps from the restored images at each value of number of iterations are also generated to help qualitative visual inspection.

The variation of PFOM, SSIM, PSNR and EPI, with respect to the number of iterations are compared in terms of their ability to quantify blurring of edge pixels during restoration, with the support of qualitative evaluation of the restored images and the binary edge map extracted from them. The correlation of the IQA and edge quality indices with Mean Opinion Score (MOS) and their features such as dynamic range are compared to prove the scope of PFOM based edge quality index to be used as a measure of edge preserving capability of non-linear filters.

Axial Plane Spin Echo Fast Spin Contrast MR images of the study MRS of series T1 SE FS+C of GlioblastomaMulti-forme (GBM) - Edema Complex are used as specimens. The specimen images were collected from Hind Labs, Government Medical College Kottayam, Kerala, India. These MR images contain Rayleigh distributed noise and weak as well as strong morphological edges. So that the efficacy of the proposed edge preservation index can be demonstrated more technically and convincingly with the help of these images. A cohort of ten MR images is used in the experiment and the experimental study is performed in Matlab®.

In this article, PFOM between the binary edge map of the original and restored image is proposed as the objective measure of the edge preservation capability offered by the restoration scheme, anisotropic diffusion in this context. PFOM [26] is an index usually used to compare the performance of different edge detection methods. Ranjani and Thiruvengadam [27] have employed PFOM to measure the edge preservation in SAR images despeckled with Dual Tree Complex Wavelet Transform (DTCWT). Different from the practice followed in this literature [27] the technique used for extracting the binary edge map of the original and the restored images is carefully formulated to reduce the noise susceptibility of the PFOM. Moreover, before employing any edge preservation metric for the objective evaluation of the non-linear spatial filters, their dynamic variability and correlation with the subjective quality ratings are evaluated.

The PFOM between the binary edge maps of the original and smoothed image is computed as [26],

$$\text{PFOM} = \frac{1}{\text{Max}(N_0, N_s)} \sum_{k=1}^{N_s} \frac{1}{1+\alpha d^2(k)} \quad (1)$$

where N_0 and N_s are the number of dominating or strong edges present in the original MR image and smoothed image respectively. ' α ' is an arbitrary penalty parameter which penalizes the misplaced edge pixels. $d^2(k)$ is the distance between the k^{th} edge pixel in the edge map of restored image and the nearest edge pixel in the edge map of the original image. The distance, $d^2 [(i,j), (m,n)]$ is the 'Euclidean derived Pythagorean distance' which is computed as,

$$d[(i,j), (m,n)] = \sqrt{(i-m)^2 + (j-n)^2} \quad (2)$$

PFOM measures the number of edge pixels diminished during smoothing and simultaneously, the number misplaced or dislocated edge pixels. The edge maps from the original MR image and smoothed image are generated via gradient based thresholding. The gradient of both noisy and restored images is computed using 'Sobel' discrete derivative kernel depicted in Fig. (1). To generate the binary maps of dominating edges in the noisy MR image and smoothed image, corresponding gradient images are 'thresholded' with respect to equal gradient thresholds. It is assumed that the pixels with local gradients above the mean of local gradients in the original image are true edge pixels and not noise contributed ones. Binary map of dominating edges in the original and smoothed image are computed as,

(a)			(b)		
-1	-2	-1	-1	0	+1
0	0	0	-2	0	+2
+1	+2	+1	-1	0	+1

Fig. (1). (a) Sobel derivative operator along x direction (b) Sobel derivative operator along y direction.

$$\hat{f}_0(x,y) = \begin{cases} 1 & \text{if } G_0(x,y) \geq G_T \\ 0 & \text{else} \end{cases} \quad \text{and} \quad \hat{f}_s(x,y) = \begin{cases} 1 & \text{if } G_s(x,y) \geq G_T \\ 0 & \text{else} \end{cases} \quad (3)$$

where the threshold G_T is the mean of local gradients of the original image. $x = \{1, 2, \dots, M\}$ and $y = \{1, 2, \dots, N\}$. for an image of size $M \times N$.

$$G_T = \frac{1}{MN} \sum_{x=1}^M \sum_{y=1}^N G_0(x,y) \quad (4)$$

G_0 and G_s are the gradient images generated from the original and smoothed image, respectively. Equation (1) – (4) implies,

$$N_0 = \sum_{x=1}^M \sum_{y=1}^N \hat{f}_0(x,y) \quad \text{and} \quad N_s = \sum_{x=1}^M \sum_{y=1}^N \hat{f}_s(x,y) \quad (5)$$

The gradient magnitude is computed from gradient along horizontal and vertical directions [28] such that,

$$G(x,y) = \sqrt{g_x^2 + g_y^2} \quad (6)$$

where the gradient along x and y directions,

$$g_x = \frac{\partial f(x,y)}{\partial x} \quad \text{and} \quad g_y = \frac{\partial f(x,y)}{\partial y} \quad (7)$$

For a smoothing kernel with ideal edge preservation, the number of dominating edge pixels in the smoothed and original image would be equal, with their spatial locations overlapping. For a perfect match of maps of dominating edges in the original and smoothed image, the PFOM is unity and a value of '0' indicates abrupt mismatch. In other words a value of PFOM, equal to unity, ensures that none of the dominating edge pixels in the original MR image is degraded or misplaced during smoothing. The commonly used values of arbitrary scaling constant ' α ' is 1/9 [29-31], 2 [27] and 0.2 [32]. There is no hard and fast constraint for setting ' α ' and appreciably $\alpha > 0$ as recommended by Evans and Liu [32]. In this work, the value of ' α ' is set to unity to make the PFOM completely dependent over the number of degraded edge pixels and the accuracy of the location of the preserved edge pixels during restoration. The proposed PFOM based edge quality index is compared with SSIM, PSNR, EPI and subjective edge quality index.

The mathematical formulation for computing EPI is [25],

$$\text{EPI} = \frac{\Gamma(\Delta s - \bar{\Delta s}, \bar{\Delta s} - \bar{\Delta s})}{\sqrt{\Gamma(\Delta s - \bar{\Delta s}, \Delta s - \bar{\Delta s}) \cdot \Gamma(\bar{\Delta s} - \bar{\Delta s}, \bar{\Delta s} - \bar{\Delta s})}} \quad (8)$$

$$\Gamma(s_1, s_2) = \sum_{i,j \in \text{ROI}} s_1(i,j) \cdot s_2(i,j) \quad (9)$$

Where $\Delta s(i,j)$ and $\bar{\Delta s}(i,j)$ are the high pass filtered version of the Region of Interest (ROI) in the reference $s(i,j)$ and its degraded or its transformed version $\bar{s}(i,j)$, obtained with a standard approximation of 3*3 Laplacian kernel. $\bar{\Delta s}$ and $\bar{\Delta s}$ are the mean of Laplacian filtered ROI in the reference and the transformed images, respectively. The SSIM [33] between the raw MR image 'X' and restored image 'Y' is given as

$$\text{SSIM}(X, Y) = \frac{(2\mu_x\mu_y + C_1)(2\sigma_{xy} + C_2)}{(\mu_x^2 + \mu_y^2 + C_1)(\sigma_x^2 + \sigma_y^2 + C_2)} \quad (10)$$

where $C_1 = (K_1 L)^2$ and $C_2 = (K_2 L)^2$, $K_1, K_2 \ll 1$. K_1 and K_2 are two arbitrary constants with values 0.01 and 0.03 respectively. $\mu_x, \mu_y, \sigma_x^2, \sigma_y^2$ and σ_{xy} are the mean brightness of original image, mean brightness of restored image, global variance of original image, global variance of restored image and covariance between original and restored images, respectively. For an image of size $M \times N$, the PSNR is given by [34],

$$\text{PSNR} = 20 \log \left(\frac{\text{Max}(X)}{\sqrt{\frac{1}{MN} \sum_{i=1}^M \sum_{j=1}^N [X(i,j) - Y(i,j)]^2}} \right) \quad (11)$$

3. RESULTS

The dynamic variability of PFOM based edge quality metric, its correlation with subjective fidelity ratings and noise susceptibility are analysed here, in comparison with EPI, SSIM and PSNR. The objective method of characterizing the optimum region of performance of non-linear filters using this edge quality metric is also detailed.

When the image is filtered with anisotropic diffusion filtering, the amount of degraded, misplaced or diminished edge pixels increases with the number of iterations, as mentioned already. The variation of PSNR, SSIM, EPI and PFOM with respect to edge degradation is analysed to check the ability of these indices to accommodate the degradation in the edge quality. In the proposed method of quantifying the extent to which true edge pixels are preserved during

restoration, the binary edge map of original and restored images are compared using PFOM. The binary edge maps of original and restored images are extracted via gradient based threshold. The original image, the gradient of original image, binary edge map of original image, diffused image, gradient of diffused image and edge map of diffused image are shown in Fig. (2a-f). The restored image depicted in the Fig. (2d) is from an anisotropic diffusion filter with a threshold of gradient modulus 15 and number of iterations equal to 5.

The variation of PFOM, SSIM and EPI with respect to the number of iterations of anisotropic diffusion is depicted in Fig. (3). Numerical values of PSNR, PFOM, SSIM and EPI between the original and restored images at different values of number of iterations are furnished in Table 1. From the Fig. (3) and Table 1, one may be misled that EPI has better dynamic variability than PFOM. EPI accounts for the extent to which the gradient is preserved, without bothering whether the high gradient is exhibited by a true edge pixel or the noise. Consequently, the EPI would have high dynamic range as it consider diminished noise pixels also. The proposed method takes only the true edge pixels into account

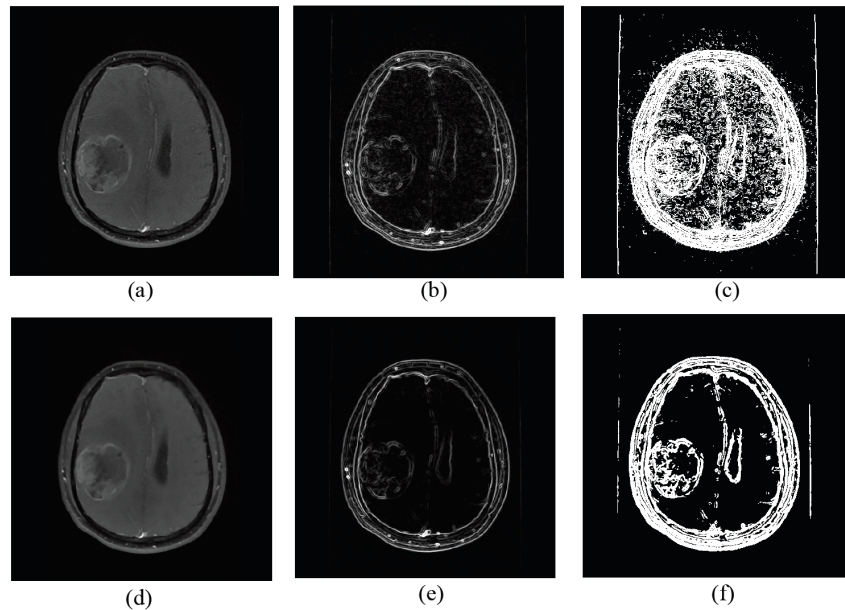


Fig. (2). (a) Original MR image (b) Gradient of original image (c) Binary edge map of original image (d) Restored image (e) Gradient of Restored image (f) Binary edge map of restored image.

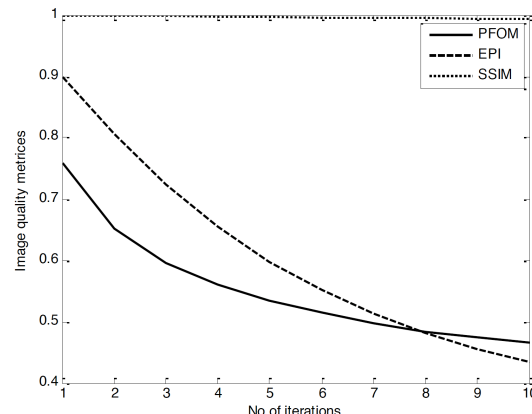


Fig. (3). Variation of PFOM, SSIM and EPI with respect to number of iterations of anisotropic diffusion.

Table 1. Numerical values of PFOM, SSIM and EPI for different values of number of iterations in anisotropic diffusion.

No of Iterations	PFOM	EPI	SSIM	PSNR	MOS
1	0.75871	0.89992	0.99957	51.32002	5
2	0.6521	0.80686	0.99897	47.52070	3.2
3	0.5957	0.72387	0.99832	45.39033	2.2
4	0.5603	0.65516	0.99766	43.95296	1.6
5	0.5345	0.59824	0.99700	42.88460	1.2
6	0.5141	0.55134	0.99636	42.04607	0.8
7	0.4975	0.51286	0.99573	41.36425	0.6
8	0.4841	0.48136	0.99513	40.79598	0.3
9	0.4739	0.45550	0.99455	40.31278	0.2
10	0.4654	0.43402	0.99399	39.89457	0

while quantifying the extent of edge preservation. Only the pixels with local gradient magnitude above the mean of local gradients are considered as true edge pixels. The threshold which is the mean gradient of the image increases with the noise level. Normally there is a possibility that noise contributed pixel intensity transitions also may be misinterpreted as true morphological edges. The feature of ‘adaptive increase in the threshold with the noise variance’ eliminates this possibility. Thus, the binary edge maps are devoid of noise contributed pseudo-edges. Hence, the proposed way of estimating the edge preservation capability of non-linear spatial filters is more robust to noise than EPI, SSIM and PSNR.

Fig. (4a-j) illustrate the changes in the binary map of the restored images with respect to the progressing number of iterations of anisotropic diffusion. From the visual inspection of binary edge maps shown in Fig. (4), it is evident that a significant change can be observed only among the first three edge maps corresponding to number of iterations equal to 1, 2 and 3. The edge maps corresponding to number of iterations 4-10, looks similar. This indicates that, the edge degradation with respect to the number of iterations is exponential. It can be confirmed in Fig. (3) that PFOM also exhibits exponential decay. This proves that the variation of PFOM is in par with subjective quality ratings than EPI does.

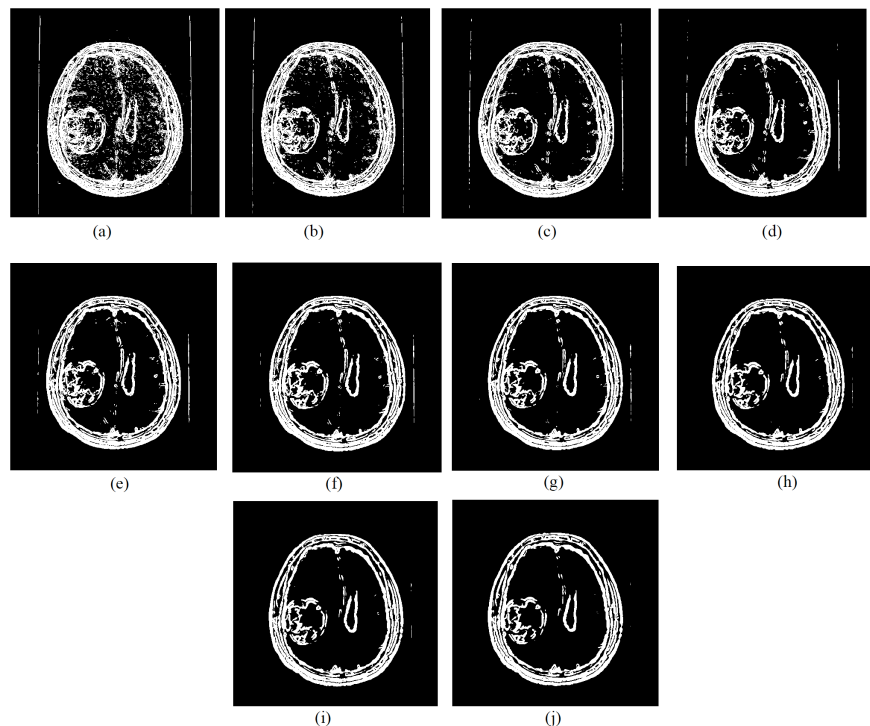


Fig. (4). Binary edge maps of the diffused images for different values of number of iterations from one to ten representing from (1st iteration (a) to 10th iteration (j)).

The restored images corresponding to the number of iterations between one and ten, illustrated in Fig. (5a-j) were shown to hundred volunteers with in the age limit 20-30. The volunteers were trained to discriminate noise pixels and true edge pixels and asked to rate the image quality in terms of the visibility of the true morphological edges with a subjective score between one and five. The Mean Opinion Score (MOS) of each image was considered as its subjective quality rating. The correlation coefficients for PFOM-MOS, EPI-MOS, PFOM-PSNR and EPI-PSNR for ten samples of test MR images are furnished in Table 2. PFOM exhibits higher correlation of 0.9998 with MOS which is only 0.9802 between EPI and MOS. For the MR image depicted in Fig. (2a) the PFOM is highly correlated with SSIM and PSNR

with coefficients 0.9245 and 0.9992, respectively. The correlation between EPI and SSIM and PSNR are 0.9779 and 0.9873, respectively. The variation of PFOM is in better correspondence with PSNR than EPI. The trial was repeated on 50 samples of MR images to confirm the PFOM has better correspondence with subjective quality rating and PSNR.

The fast decay of PFOM at the early iterations, visible in Fig. (3) is because of the fast suppression of noise pixels. The exponential region of the curve represents that no more noise pixels are left and only true edge pixels remain in the image. Therefore, the exponential region of the graph showing the variation of PFOM with respect to the change in certain operational parameters of the non-linear filters indicates

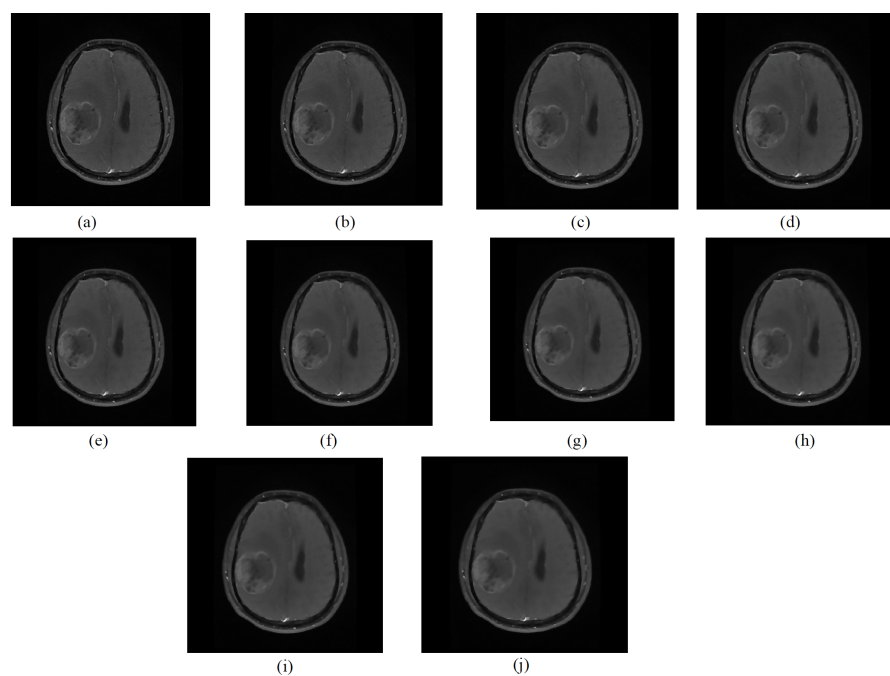


Fig. (5). The diffused images for different values of number of iterations from one to ten representing from (1st iteration (a) to 10th iteration (j)).

Table 2. Correlation coefficient of PFOM and EPI with MOS and PSNR on test images.

S.No.	Correlation Coefficient			
	PFOM-MOS	EPI-MOS	PFOM-PSNR	EPI-PSNR
Image 1	0.9998	0.9802	0.9992	0.9873
Image 2	0.9893	0.9703	0.9967	0.9831
Image 3	0.9959	0.9814	0.9991	0.9870
Image4	0.9956	0.9801	0.9975	0.9846
Image5	0.9892	0.9750	0.9978	0.9863
Image6	0.9923	0.9801	0.9988	0.9863
Image7	0.9889	0.9734	0.9938	0.9817
Image8	0.9907	0.9801	0.9927	0.9798
Image9	0.9981	0.9820	0.9974	0.9788
Image10	0.9985	0.9821	0.9989	0.9869

the optimum range of the operational parameter, at which noise suppression and the edge preservation are at the best trade off. It can be observed in the binary edge map of restored images, illustrated in Fig. (4a-j) that the noise pixels are not fully removed when the number of iterations is less than four. The shape of the PFOM curve in Fig. (3) is exponential when the number of iterations is between three and five, typically at 4. This reveals that a good trade-off between the noise removal and edge preservation is possible only with the parameter setting at exponential region of the PFOM curve. Noise removal and edge preservation are two mutually exclusive factors.

From the Table 1 it is apparent that the SSIM has limited dynamic range between 0.99957 and 0.99399. But the visual examination of the edge maps available in Fig. (4) and restored images in Fig. (5) confirms that significant difference is there among these images. The dynamic range exhibited by SSIM is not sufficient to accommodate these significant visual changes. Even though, PSNR to a certain extent accommodates these visual changes, it does not have a standard range of zero to one, like SSIM. The reliability of SSIM is doubtful in heavily corrupted images and PSNR do not comply with subjective quality ratings. Moreover, SSIM and PSNR are measures of similarity of two images and do not specifically quantify the resemblance of the edge content.

4. DISCUSSIONS

The indices for objective evaluation of non-linear filters, available in literature, HMD [8], HME [10] and DEI [13] quantify the homogeneity of the despeckled image but do not account for the extent to which edges are preserved. The coincidence of homogenous regions in the original and restored images is assessed in them. But in the proposed PFOM based edge preservation metric, the coincidence of binary maps of the true edges in the original and restored images are evaluated directly. Hence, the proposed metric directly account for the edge preservation capability of the non-linear filters. DSL [11] need a noise free reference which is difficult to provide, whereas the proposed metric use the available noisy image itself as reference. The index suggested in literature [9] is a non-reference one. But, the edges preserved during non-linear restoration have to be identified by comparing the binary edge map of the original and restored images as done in the proposed PFOM based edge preservation metric. The methods for the objective evaluation of non-linear filters available in literature [8-13] are exclusively for SAR images. Contrarily, the method suggested in this article is exclusive for medical imagery, especially, MR images.

PFOM had been used by Ranjani and Thiruvengadam [27] to measure the edge preservation capability of DTCWT despeckling. However, the noise robustness of the PFOM based edge preservation metric depends on the efficiency of the method employed for extracting the binary edge maps from the original and restored images. The sharp pixel intensity transitions, seen on the image could be either true morphological edges or noise contributed ones. Unless, the edge detection method is able to extract the binary map of true morphological edges, excluding the noisy pixel intensity transitions, the PFOM edge preservation metric becomes

susceptible to noise level. In the gradient based threshold used in this article for edge detection, the threshold adaptively shifts up, as the level of noise increases. The feature of noise adaptive threshold makes the PFOM based edge preservation metric robust to noise level. In addition, the procedure for identifying the optimum values of the operational parameters of non-linear filters has been practically demonstrated. It is observed that the exponential region of the PFOM versus operational parameter curve offers the best trade-off between the noise suppression and edge preservation. The correlation of the PFOM based edge preservation metric with subjective edge quality assessment has been proven both qualitatively and quantitatively. One of the major demerits of the Laplacian kernel used in EPI [21-25] is enhancement of noise and Laplacian is a sharpening or high pass filter kernel. The proposed PFOM based kernel is observed to be superior to EPI for its noise robustness and correlation with qualitative edge fidelity ratings.

5. CONCLUSION

Objective indices to quantify the edge preservation capability of the non-linear filters are necessary for the comparison of their performance and to find out the optimum value of their operational parameters. The edge quality indices so far available are not in good agreement with the subjective quality ratings and are sensitive to noise. An edge quality index was proposed and an objective method to evaluate the edge preservation offered by the non-linear spatial filters was demonstrated using this index.

The proposed PFOM based edge quality measure complies well with subjective quality ratings than SSIM, PSNR and EPI. PFOM exhibits higher correlation of 0.9998 with MOS which is only 0.9802 between EPI and MOS. It has a standard range between zero and one as SSIM and better dynamic variability than SSIM. For a range of number of iterations of the AD filter from one to ten, SSIM exhibited a dynamic range of 0.99957-0.99399 and PFOM exhibited a better dynamic range of 0.4739-0.75871.

The proposed PFOM based edge preservation metric is superior to SSIM and EPI in terms of robustness to noise, correspondence with subjective fidelity ratings and dynamic range. Moreover, the proposed PFOM based edge quality index has good agreement with PSNR also. The metric can also be used as a stopping criterion in iterative smoothing.

CONFLICT OF INTEREST

The authors confirm that this article content has no conflict of interest.

ACKNOWLEDGEMENTS

One of the authors would like to thank the fund from the DST-FIST, Govt of India, vide Ref.: SR/FST/College-189/2013, Dated: 6th August 2014.

REFERENCES

- [1] Mingliang X, Pei L, Mingyuan L, et al. Medical image denoising by parallel non-local means. Neurocomputing 2016; doi:10.1016/j.neucom.2015.08.117.

- [2] Manjon JV, Coupe P, Buades A. MRI noise estimation and denoising using non-local PCA. *Med Image Anal* 2015; 22(1): 35-47.
- [3] Ai D, Yang J, Fan J, Cong W, Wang X. Denoising filters evaluation for magnetic resonance images. *Optik* 2015; 126(23): 3844-50.
- [4] Liu Y, Ma C, Clifford BA, Lam F, Johnson CL, Liang ZP. Improved low-rank filtering of magnetic resonance spectroscopic imaging data corrupted by noise and field inhomogeneity. *IEEE T on Bio-Med Eng* 2016; 63(4): 841-9.
- [5] Akar SA. Determination of optimal parameters for bilateral filter in brain MR image denoising. *Appl Soft Comput* 2016; 43: 87-96.
- [6] Hong Y, Ren G, Liu E. A no-reference image blurriness metric in the spatial domain. *Optik* 2016; <http://dx.doi.org/10.1016/j.jleo.2016.03.077>.
- [7] Molina CL, De Baets B, Bustince H. Quantitative error measures for edge detection. *Pattern Recogn* 2013; 46(4): 1125-39.
- [8] Zhang Y, Cheng HD, Huang J, Tang X. An effective and objective criterion for evaluating the performance of denoising filters. *Pattern Recogn* 2012; 45(7): 2743-57.
- [9] Gómez L, Buemi ME, Jacobo-Berlles JC, Mejail ME. A new image quality index for objectively evaluating despeckling filtering in SAR images. *IEEE J-STARS* 2016; 9(3): 1297-1307.
- [10] Zhang Y, Cheng HD, Huang J, Tang X. A novel metric for image denoising algorithms. *Intelligence Science and Big Data Engineering* 2013; 8261: 538-45.
- [11] Yang X, Wu K, Tang Y. A new metric for measuring structure-preserving capability of despeckling of SAR images. *ISPRS J Photogramm* 2014; 94: 143-59.
- [12] Zhao Y, Liu JG, Zhang B, Hong W, Wu YR. Adaptive total variation regularization based SAR image despeckling and Despeckling Evaluation Index. *IEEE T Geosci and Remote* 2015; 53(5): 2765-74.
- [13] Dellepiane SG, Angiati E. Quality assessment of despeckled SAR images. *IEEE J-STARS* 2014; 7(2): 691-707.
- [14] Zhang L, Zhang L, Mou X, Zhang D. FSIM: a feature similarity index for image quality assessment. *IEEE Trans on Image Process* 2011; 20(8): 2378-86.
- [15] Wang Z, Bovik AC. A universal image quality index. *IEEE Signal Process Lett* 2002; 9(3): 81-4.
- [16] Yim C, Bovik AC. Quality assessment of de-blocked images. *IEEE Trans on Image Process* 2011; 20(1): 88-98.
- [17] Brooks AC, Zhao X, Pappas TN. Structural similarity quality metrics in a coding context: exploring the space of realistic distortions. *IEEE Trans on Image Process* 2008; 17(8): 1261-73.
- [18] Wang Z, Li L, Wu S, Xia Y, Wan Z, Cai C. A new image quality assessment algorithm based on SSIM and Multiple Regressions. *Int J Sig Process, Image Process Pattern Recogn* 2015; 8(11): 221-30.
- [19] Pei SC, Chen LH. Image quality assessment using human visual DOG model fused with random forest. *IEEE Trans on Image Process* 2015; 24(11): 3282-92.
- [20] Li C, Bovik AC. Content-partitioned structural similarity index for image quality assessment. *Signal Process Image Commun* 2010; 25(7): 517-26.
- [21] Soni V, Bhandari AK, Kumar A, Singh GK. Improved sub-band adaptive thresholding function for denoising of satellite image based on evolutionary algorithms. *IET Signal Process* 2013; 7(8): 720-30.
- [22] Ramadan ZM. A new method for impulse noise elimination and edge preservation. *Can J Elect Comput E* 2014; 37(1): 2-10.
- [23] Satyanarayanan M. Edge analytics in the internet of things. *IEEE PervasComput* 2015; 14(2): 24-31.
- [24] Kang J, Lee J, Yoo Y. A New Feature-enhanced Speckle Reduction Method based on Multiscale Analysis for Ultrasound B-mode Imaging. *IEEE T Bio-Med Eng* 2015; 99:1-10.
- [25] Sattar F, Floreby L, Salomonsson G, Lovstrom B. Image enhancement based on a nonlinear multiscale method. *IEEE Trans on Image Process* 1997; 6:888-95.
- [26] Pratt WK. *Digital Image Processing*. 4th ed. New York: Wiley 1977.
- [27] Ranjani JJ, Thiruvengadam SJ. Dual-tree complex wavelet transform based SAR despeckling using inter-scale dependence. *IEEE T Geosci Remote* 2010; 48(6): 2723-31.
- [28] Gonzalez RC, Woods RE. *Digital Image Processing*. 3rd ed. New Jersey: Pearson Prentice Hall 2008.
- [29] Agaian SS, Panetta KA, Nercessian SC, Danahy EE. Boolean derivatives with application to edge detection for imaging systems. *IEEE Trans Syst Man Cybern B* 2010; 40(2): 371-82.
- [30] Bao P, Zhang L, Wu X. Canny edge detection enhancement by scale multiplication. *IEEE T Pattern Anal* 2005; 27(9): 1485 -90.
- [31] Trahanias P, Venetsanopoulos A. Vector order statistics operators as color edge detectors. *IEEE Trans Syst Man Cybern B* 1996; 26(1): 135-43.
- [32] Evans AN, Liu XU. A morphological gradient approach to color edge detection. *IEEE Trans on Image Process* 2006; 15: 1454-63.
- [33] Wang Z, Bovik AC, Sheikh HR, Simoncelli EP. Image quality assessment: from error visibility to structural similarity. *IEEE Trans on Image Process* 2004; 13: 600-12.
- [34] Thu QH, Ghanbari M. Scope of validity of PSNR in image/video quality assessment. *Electron Lett* 2008; 44:800-801.